# Classes of Hydration Sites at Protein-Water Interfaces: The Source of Contrast in Magnetic Resonance Imaging

Seymour H. Koenig
Relaxometry Inc., Mahopac, New York 10541; and Department of Radiology, Dartmouth-Hitchcock Medical Center, Hanover, New Hampshire 03755 USA

ABSTRACT Immobilized protein solute, ~20 wt %, alters the longitudinal and transverse nuclear magnetic relaxation rates $1/T_1$ and $1/T_2$ of solvent water protons in a manner that makes their values indistinguishable from those of a typical human tissue. There is now a quantitative theory at the molecular level (S. H. Koenig and R. D. Brown III (1993) *Magn. Reson. Med.* 30:685–695) that accounts for this, as a function of magnetic field strength, in terms of several distinguishable classes of water-binding sites at the protein-water interface at which significant relaxation and solute-solvent transfer of proton Zeeman energy occur. We review the arguments that these several classes of sites, characterized by widely disparate values of the resident lifetimes $\tau_M$ of the bound waters, are associated with different numbers of hydrogen bonds that stabilize the particular protein-water complex. The sites that dominate relaxation–and produce contrast in magnetic resonance imaging (MRI), which derives from $1/T_1$ and $1/T_2$ of tissue water protons–have $\tau_M \approx 10^{-6}$ s. These, which involve four hydrogen bonds, occupy ≤1% of the protein-water interface. Sites that involve three bonds, although more numerous, have ≤20% smaller intrinsic effect on relaxation. The greater part of the "traditional" hydration monolayer, with even shorter-lived hydrogen-bonded waters, has little influence on solvent relaxation and is relatively unimportant in MRI. Finally, we argue, from the data, that most of the protein of tissue (a typical tissue is mostly protein) must be rotationally immobile (with Brownian rotational relaxation times slower than that of a $5 \times 10^7$ Da (very heavy) globular protein). We propose a functional basis for this immobilization ("cytoplasmic order"), and then indicate a way in which this order can break down ("cytoplasmic chaos") as a result of neoplastic transformation (cancer) and alter water-proton relaxation rates of pathological tissue and, hence, image contrast in MRI.

## INTRODUCTION

The increasing utility of magnetic resonance imaging (MRI) in diagnostic medicine has stimulated research into the mechanisms that relax the magnetic moments of the protons of tissue water. Given that such images are reconstructed from nuclear magnetic resonance (NMR) signals of tissue-water protons, and that the water contents of most tissues are close to equal, each clinical image is, in essence, a map of the spatial- and hence tissue-dependent values of the longitudinal ($1/T_1$) and transverse ($1/T_2$) proton relaxation rates, with relative weightings determined by clinical considerations. Hence the importance of understanding the mechanisms of nuclear relaxation of water in tissue if one wants fundamental insights into the basis of contrast in MRI and, ultimately, its relation to disease.

Several important generalities regarding the mobility of water in tissue have come from the initial work in this area (cf. Koenig et al., 1984; Koenig and Brown, 1985, 1988). First, the widths and integrated intensities of the proton signals in MRI show that, certainly to first order, all tissue water is highly mobile, differing little in its dynamic properties from pure water. Second, extensive data on the dependence of the proton $1/T_1$ on the static magnetic field $B_0$ show–again, to first order–that the range of water diffusion is sufficiently great that tissue water molecules can explore their intra- and extracellular environments within a relaxation time, so that the measured relaxation rates are grand averages of the local molecular-level interactions that induce relaxation. Third, these interactions are indeed local, in time and in space; relaxation takes place during the physical encounters of tissue-water molecules with the surfaces of solute macromolecules, with the water dynamics and structure being appreciably perturbed only within atomic dimensions of an encounter event. Fourth, because the solids content of most tissue types (excluding those with significant lipid content) is predominantly protein, it might be expected that protein solutions are models for relaxation in tissue. This is indeed the case, provided that the solute protein is immobilized. Current understanding (Koenig and Brown, 1993) can be summarized by noting that two samples, one a typical tissue and another a sample of immobilized protein, ~100 kDa, and of comparable solids content, cannot be distinguished by measurement of any relaxation parameter of the samples (including $1/T_1$, $1/T_2$, or $1/T_{1\rho}$, the "relaxation rate in the rotating frame"), including their dependence on magnetic field and temperature. This is a remarkable finding, and is true whether the protein is immobilized by thermal denaturation (Koenig and Brown, 1988, 1991); chemical cross-linking (Lester and Bryant, 1991; Bryant et al., 1991; Koenig and Brown, 1993); protein-protein "crowding" at high solute densities for certain proteins (Beaulieu et al., 1989; Koenig et al., 1992; Koenig

*Received for publication 23 January 1995 and in final form 26 April 1995.*
Address reprint requests to Dr. Seymour H. Koenig, Relaxometry Inc., P.O. Box 760, Mahopac, NY 10541. Tel.: 914-628-7957; E-mail: balony@watson.ibm.com.

0006-3495/95/08/593/11 $2.00

et al., 1993a, b); or extensive dehydration (Schauer et al., 1988, as shown in Fig. 2 of Koenig et al., 1993c).

It is now established that relaxation of water protons in protein solutions and in tissue is dominated by interactions at particular protein-water interfacial sites that cover <1% of the protein-water interface (Koenig et al., 1993c; Koenig and Brown, 1993). These are sites that hold solvent water molecules in the first hydration layer for ~1 μs (a relatively long time), ostensibly by four hydrogen bonds. Shorter-lived complexes, in greater density but with less impact on relaxation rates, have also been discussed (Koenig and Brown, 1993). The majority of the "traditional hydration shell," the water monolayer that covers the majority of the interface, was shown quite early to have little influence on water-proton relaxation rates (Koenig and Schillinger, 1969; Koenig, 1980). The supporting data are nuclear magnetic relaxation dispersion (NMRD) profiles, which indicate the magnetic field dependence of $1/T_1$ of the protons of the mobile water molecules of tissue and of protein solutions, and their variation with temperature $T$. Measurement of these profiles, development of the instrumentation (still only available in but a small number of laboratories worldwide), and extension and application of theory constitute the specialty now called "relaxometry"; the instrumentation required is a field-cycling relaxometer (Redfield et al., 1968; Noack, 1986; Koenig and Brown, 1987). Only a limited amount of analogous deuteron NMRD data exist, but their impact has been seminal in leading to the present understanding of mechanism (Koenig et al., 1993c). The major point is that water protons are relaxed predominantly by other protons; for solutions of native protein, this means, mainly, other water protons; but for immobilized protein and for tissue, those interactions that transfer proton magnetization between solute and solvent predominate. Such transfer is of little import for deuterons, with magnetic moments that are relaxed 10-fold more effectively than are protons because of deuteron electric quadrupolar interactions, a nuclear relaxation mechanism that is insensitive to local magnetic fields. It was by comparison of proton and deuteron $1/T_1$ NMRD profiles for the same samples that the "hydrodynamic" and "magnetization transfer" contributions could be distinguished and a unified overall picture recently derived (Koenig and Brown, 1993).

The aim of this review is to codify the scattered data, reinterpreting some of it (Hallenga and Koenig, 1976) to present a coherent review of how a small fraction of the protein hydration layer leads to the observed contrast between differing tissues in MRI. The approach is to present broad, interrelated principles, using qualitative but robust arguments from published data, together with references to the defining experiments from which detailed quantitative understanding can be obtained. In addition to their relevance to MRI, the results have their own intrinsic value, since they clarify several issues in terms of fundamental magnetic interactions at the molecular level, including their quantitative dependence on the dynamic nature of protein hydration and on the molecular dynamics of water in tissue.

## BACKGROUND

### The concept of motional narrowing

$1/T_1$ and $1/T_2$ of the nuclei of liquids characterize the rapidity with which a thermodynamic ensemble of similar nuclei attains thermal equilibrium. For partially deuterated water, e.g., every solvent deuteron or proton must be coupled to the thermal background, the "lattice," through a noisy interaction modulated by Brownian thermal motion, which conveys the lattice temperature to the nuclear ensemble. For liquid water (and isotropic liquids generally), the mechanism of "motional narrowing" (Bloembergen et al., 1948; Solomon, 1955) dominates relaxation: a given water proton, for example, senses the local dipolar magnetic field generated by nearby water protons. This field fluctuates rapidly in magnitude and orientation (at rates $\sim 10^{12}\ s^{-1}$, the "correlation frequency" $\nu_c$) because of the normal, rapid Brownian rotation and translation of water molecules–so rapidly, in fact, that the proton-proton interaction is essentially averaged out. More specifically, the Fourier components of the noisy interaction are weak, are broadly and uniformly distributed from very low frequencies up to near $\nu_c$, and decrease toward 0 at higher frequencies ("pink" noise). These Fourier components of the magnetic noise (for protons) induce transitions among the orientational Zeeman energy levels of the coupled protons, changing the overall magnetization of the ensemble; hence (at least, intuitively), relaxation. (For the usual set of simplifying assumptions regarding the random processes that generate the noise, the noise spectrum as a function of frequency $\nu$ is Lorentzian; i.e., of the general form $\tau_c/(1 + (2\pi\tau_c\nu)^2)$, where $2\pi\tau_c = 1/\nu_c$, assumptions entirely adequate for what follows. An important property of a Lorentzian is that its integral over all $\nu$ is independent of $\nu_c$, its value (the total noise power) being proportional to absolute temperature.)

Two important results for motionally narrowed conditions are: for $B_0 \to 0$, $1/T_1 \to 1/T_2$, and for $B_0 \to \infty$, $1/T_1 \to 0$ and $1/T_2 \to 0.3/T_2(B_0 = 0)$, provided $\nu_c$ is independent of $B_0$, as it generally is in diamagnetic systems. In reality, $1/T_1$ and $1/T_2$ are two components of the same physical tensor quantity which, when the system is isotropic (e.g., for isotropic liquids when $B_0 = 0$), become equal. At high fields, $1/T_2$ is a measure of the low-field $1/T_1$, an important consideration for MRI (see below). When motional narrowing is not applicable–as in the solid state–$1/T_1$ and $1/T_2$ are unrelated.

For protons of pure water, the averaging is so effective that several seconds ($1/T_1 \approx 0.3\ s^{-1}$ at 25°C) are required for the proton ensemble to reach thermal equilibrium, "narrowed" from a proton-proton interaction $\sim 10^5\ s^{-1}$. For the present purposes, it is only necessary to realize that slowing of the rotational motion of a water molecule will increase the intrinsic relaxation rates of water protons proportionately. For example, reducing $\nu_c$ of a given water molecule to $\sim 10^7\ s^{-1}$ increases the relaxation rates of its protons $10^5$-fold, something that might be accomplished, e.g., by bind-

ing a water molecule irrotationally to a macromolecule of ~500 kDa. For protons of protein-bound waters, as well as for protein protons, motional narrowing theory holds for molecular weights $\leq 5 \times 10^7$ Da, the upper limit being rarely encountered for native protein.

The deuteron magnetic moment is about one-sixth that of the proton, leading to relaxation rate contributions from magnetic interactions ~3% of that of a proton in the same local field. However, as noted, the deuteron has a significant electric quadrupolar moment that couples to the lattice through the gradients of the electric field at the deuteron position (an interaction relatively insensitive to whether the water is bound or free, and to $B_0$ as well). For motional-narrowing conditions, the theory of quadrupolar relaxation is formally identical to relaxation by magnetic dipolar interactions; $1/T_1$ for deuterons is about eightfold greater than for protons at 25°C.

### The heterogeneous "two-site" exchange model

It has been known for three decades that diamagnetic solute protein increases $1/T_1$ and $1/T_2$ of solvent water protons (Daszkiewicz et al., 1963). (Relaxation by metalloproteins containing paramagnetic metal ions is a separate subject entirely, and of no relevance here.) These authors attributed the increases, observed in ovalbumin solutions at 0.33 T (14 MHz proton Larmor frequency $\nu$) and 20°C, to specific binding of solvent water at the protein-water interface. They assumed a "two-site" exchange model, in which waters are bound at the protein-water interface with sufficient rigidity to sense the rotational thermal (Brownian) motion of solute protein, yet are in sufficiently rapid exchange with solvent so that changes in the relaxation rates of protons of the bound waters are communicated to the bulk solvent, the source of the NMR signal. The magnitude of the phenomena, of course, depends on the fraction of the interfacial area covered by sites that satisfy these criteria, and on the enhancement of the proton relaxation rates when the waters are protein-bound. This enhancement is dominated by the increase in $\nu_c$ upon binding, which can only be deduced from measurements of relaxation over a significant range of $B_0$, i.e., from NMRD profiles.

Values of $\nu_c$ for protein solutions were first reported for (demetalated) apotransferrin, a highly aspherical serum protein of ~85 kDa; Koenig and Schillinger (1969) measured water-proton $1/T_1$ NMRD profiles from 0.01–50 MHz for a wide range of protein concentration, solution pH and ionic strength, and sample temperature. The solvent was partially deuterated in one case. Within the context of a two-site model, three unequivocal conclusions were reported: 1) "the lifetime [$\tau_M$] on the protein molecules of the exchanging entities, whether entire water molecules or individual protons, is in the range 0.1 to 10 $\mu$s"(p. 3283); 2) from the insensitivity of the NMRD profiles to pH, from the upper bounds on $\tau_M$ derived from the magnitudes of the profiles, and from quantitative arguments regarding the calculated lifetimes of individual interfacial protons due to acid- or base-catalyzed exchange near neutral pH, two-site exchange required that entire water molecules be the entities in rapid exchange; and 3) "the number of water molecules involved is a small fraction of the number usually considered to be in the first hydration shell." (p. 3283) However, it was not until very recently (Koenig et al., 1993c) that a small number of 1-$\mu$s interfacial binding sites (corresponding to $\nu_c \approx 0.1$ MHz) was demonstrated for several different proteins, including BSA powder, hydrated to about four monolayers (see below). In the interim, an assiduous search for hydrodynamic mechanisms, rather than exchange, was carried out (Koenig et al., 1975; Hallenga and Koenig, 1976), but with scant success.

The two-site exchange contribution of a given class of binding site to $1/T_1$ disperses to (approaches) 0 for $\nu \gg \nu_c$. From the high-field contribution of solute apotransferrin, an initial estimate gave $\nu_c$ ~50 MHz, and it appeared (Koenig and Schillinger, 1969) that ~20% of the hydration layer is involved, with $\tau_M \sim 2 \times 10^{-9}$ s. With more–and improved–data for additional proteins, this density was revised upward to ~30% of the protein surface, with $\tau_M \sim 4 \times 10^{-10}$ s, and the waters conjectured to be associated with charged amino acids at the protein surface (Koenig, 1980). Thus, the earliest $1/T_1$ NMRD data on protein solutions indicated a heterogeneous solute-solvent interface: at least two classes of hydration sites were reported for protein-water solutions, with widely differing values of $\tau_M$ and numerical densities. As will be shown, there are others.

## DATA SHOWING SPECIFIC CLASSES OF SITES

### Demonstration and nature of the 1-$\mu$s sites

#### *Results from deuteron NMRD profiles*

As already noted, the earliest proton $1/T_1$ NMRD data for apotransferrin (Koenig and Schillinger, 1969), when interpreted in terms of two-site exchange, indicated the existence of a class of site with $\tau_M$ in the range 0.1–10 $\mu$s. Moreover, in that early work, and in more recent work as well (Koenig and Brown, 1993), measurements as a function of pH were made; these, together with kinetic arguments regarding acid- and base-catalyzed proton exchange, were used to conclude that entire water molecules were the exchanging species. However, it is only very recently (Koenig et al., 1993c) that the lifetime and interfacial density of this class of site (and others) have been established. Fig. 1 shows representative deuteron and proton profiles that led to these conclusions (Fig. 1, *open* and *filled symbols*, respectively) for native and chemically cross-linked BSA, ~11 wt % (~1.5 mM), at 35°C.

The deuteron data for native BSA are considered first. Deuteron data are more difficult to obtain, and therefore noisier, than data for protons; the deuteron magnetic moment is sixfold smaller, and (in a field-cycling relaxometer) the intrinsic signal sixfold lower. Moreover, the greater intrinsic relaxation rates of deuterons often cause signal to

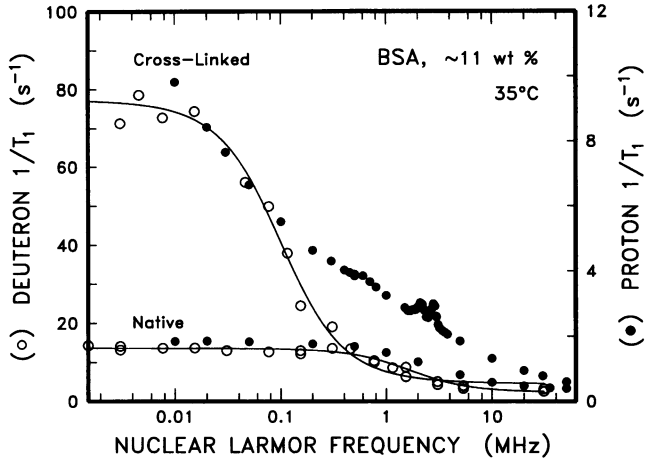


FIGURE 1 Representative deuteron (○) and proton (●) $1/T_1$ NMRD profiles of samples of native and chemically cross-linked BSA in isotopically mixed solvent, at 35°C. The intent is to demonstrate the similarity of the deuteron and proton profiles for native protein, and the remarkable distinctions between the analogous profiles for glutaraldehyde-cross-linked samples (see text). The deuteron data are for 12 wt % BSA, with the solution 54% deuterated, at 35°C (after Koenig et al., 1993c). The proton data are for 10 wt % BSA, 54% deuterated solvent (after Koenig et al., 1993d). The solid curves through the deuteron data are single near-Lorentzian profiles, here used to help visualize the data (Hallenga and Koenig, 1976).

be lost as $B_0$ is switched during the measurement field cycle. A general rule is that deuteron and proton signals tend to be of comparable magnitude in solvent that is 90% deuterated.

The solid curve through the deuteron profile for the native sample, Fig. 1, is somewhat broader than a single Lorentzian, the curve expected from motional narrowing theory and a two-site exchange model (cf. Hallenga and Koenig, 1976). It is computed for $\nu_c \approx 1.7$ MHz, very close to the rotational diffusive relaxation time calculated for BSA molecules using Stokes' law (Koenig and Brown, 1991). The agreement of the curve with the data is clearly quite good (but can be improved; see below). Since for deuterons in pure water at 35°C, $1/T_1 \approx 1.8\ s^{-1}$, the low-field rate enhancement in this sample is about sevenfold despite a change in correlation frequency upon binding from $\nu_c \approx 5 \times 10^{10}\ s^{-1}$ to $1.7 \times 10^6$, a factor of $\sim 3 \times 10^4$. Hence the fraction of waters bound is $(7/3 \times 10^4) \approx 2.3 \times 10^{-4}$, corresponding to 12 mM (water is 55 M). Since the protein is 1.5 mM, this means that about eight water molecules rigidly bound to each solute BSA molecule and characterized by a correlation frequency near 1.7 MHz (since the curve is not grossly broader than a Lorentzian) can explain the NMRD data, provided that each is in sufficiently, but not too, rapid exchange with solvent. A simple calculation shows that there is space for ~800–1000 water molecules in a monolayer at the BSA-water interface, so that only ~1% of the protein surface is needed to account for the deuteron $1/T_1$ profile for native BSA, in this first order analysis, which is refined below.

Limits can be placed on the value of $\tau_M$ for these waters: $\tau_M$ must be longer than $4 \times 10^{-8}$ s (40 ns) to allow bound waters to sense the 1.7 MHz value of $\nu_c$ (the conversion is $\sim 1/11\nu_c$ (Koenig and Schillinger, 1969; Koenig and Brown, 1991)) and shorter than the deuteron $T_1$ on the protein, readily estimated to be $2 \times 10^{-5}$ s (20 $\mu$s) (from the change in $\nu_c$ upon binding). This range of almost three orders of magnitude hardly defines $\tau_M$; its actual value comes directly from the inflection in the profile for the cross-linked sample (Fig. 1). The immediate question becomes: what fluctuation mechanism generates $\nu_c$, ≈0.1 MHz, for this sample (the actual native sample, after cross-linking), given that cross-linking ostensibly halts all significant rotational thermal motion of the protein? The answer, only recently proposed (Koenig et al., 1993c), is that it is a reflection of $\tau_M$: repeated binding of water molecules interrupts the rapidly fluctuating, highly narrowed interactions that relax deuterons in the solvent, and substitutes a series of square pulses of noise of mean length $\tau_M \approx 10^{-6}$ s (1 $\mu$s) and magnitude that depend on both the binding geometry and the orientation of the protein-water complex with respect to the direction of $B_0$, thereby enhancing relaxation. The solid curve through the data is again a single near-Lorentzian, and once again the fit is very good, establishing the existence of 1-$\mu$s sites, which dominate the profile.

### *Results from proton NMRD profiles: magnetization transfer*

For native BSA (Fig. 1) the proton profile (Fig. 1, *filled symbols*) resembles quite closely that for deuterons, as expected from earlier data for other proteins (Hallenga and Koenig, 1976; Koenig et al., 1978). Note, however, that the actual rates are quite different, reflecting in part the eightfold lower intrinsic relaxation rates of protons compared with deuterons in pure water at 35°C. There is also a small contribution to the proton relaxation rate, for BSA, which arises from the interactions of the protons of bound water with protein protons. (This contribution increases with the molecular weight of the solute native protein; its phenomenology has been discussed (Koenig and Brown, 1991).) Again, only limits on $\tau_M$ for native BSA can be gotten from these data: the short-time limit is the same as that derived for deuterons, since the values of $\nu_c$ are (perforce) the same, and the long-time limit is shortened about eightfold, still hardly informative.

It is the proton profile for cross-linked BSA that is qualitatively different from all the others (Fig. 1), in several aspects, three of which are clear in Fig. 1. First, it is highly non-Lorentzian, not at all similar in functional form to the deuteron profile for the analogous sample nor to the deuteron and proton profiles of native BSA. Second, if a value of $\nu_c$ exists that characterizes the data, it is off-scale to the left. Third, there are three peaks in the data (Winter and Kimmich, 1982a,b; Kimmich et al., 1986), two larger ones at 2.2 and 2.8 MHz, and a smaller but visible "difference peak" near 0.6 MHz. (More extensive data on this phenomenon are in Fig. 5 of Beaulieu et al., 1989.) Other differences have also been noted (Koenig et al., 1993c): the dependence on temperature is much reduced, and the high-

field value of $1/T_2$ is much increased. A quantitative theory that encompasses all these points has been given (Koenig and Brown, 1993) based on the essential change in the mechanisms of solvent proton relaxation brought on by immobilizing solute protein. Here we emphasize its qualitative aspects as they relate to several classes of water-binding sites on protein, i.e., to an intrinsic heterogeneity of protein hydration.

Once protein is immobilized, relaxation of its protons is no longer described by motional-narrowing theory (which, as noted, is appropriate for protons of solvent and mobile protein); solid-state concepts apply, and, because of an enhanced transfer of magnetization between protein and water protons, the solid-state aspects are reflected in the water NMRD profiles. This enhancement is due to a decrease in the $\nu_c$ value of the interaction of protein protons with water protons which, for BSA, drops from 1.7 to 0.10 MHz. For the solid state, the essence of proton relaxation that arises from proton-proton interactions is that mutual proton spin-flips contribute to a relatively rapid, lossless diffusive spread of proton magnetization throughout the solid (immobilized protein in this case). $1/T_2$ is short ($\sim 10^{-5}$ s, determined by the proton-proton interaction energy), and $1/T_1$ is long (because it requires energy loss); it is dominated by other mechanisms, often chance "relaxation sinks" in the system. For protons in immobilized solute protein, one set of sinks comprises the NH (amino) groups on every amino acid throughout the protein, now accessible to solvent magnetization because of enhanced magnetization transfer and diffusion. The $^{14}N$ nuclear levels are split statically by electric quadrupolar interactions, with two levels differing by 2.2 and 2.8 MHz from the ground state (and rather insensitive to $B_0$), and are estimated to relax rapidly (Koenig, 1988). When the Zeeman energies of the NH protons match possible transitions among the $^{14}N$ levels, there is rapid relaxation of these protons, which in turn become sinks, and sources, of magnetization for the Zeeman reservoir of protein protons; hence the three peaks in the data (Fig. 1). The other major class of sinks involves the 1-$\mu$s sites; these not only relax the protons of waters bound to protein, and transfer proton magnetization between water and protein, these sites are the dominant relaxation sinks–and therefore, the major determinant of $1/T_1$–for protein protons in these immobile systems over most of the range of $B_0$. The foregoing arguments describe, qualitatively, aspects of the proton data for cross-linked protein; better quantitation requires consideration of another class of sites (see below).

## Demonstration of 23-ns sites

### *Results from deuteron NMRD profiles of BSA*

The fit of the two curves that describe the deuteron data (Fig. 1) is not quite adequate in three ways: the ratio of the low-field rates should be equal to the ratio of the $\nu_c$ values (17:1); the curves are broader than single Lorentzians; and the agreement in the field range 0.5–10 MHz could be improved (the vertical scale must be expanded to see this (Koenig and Brown, 1993)). Postulating 23-ns sites, with a density about seven times that of the 1-$\mu$s sites, resolves these three problems favorably. With only four constants, i.e., the lifetimes and densities of these two classes of interfacial binding sites, it then becomes possible to describe the two deuteron NMRD profiles with two Lorentzians, including their relative amplitudes, within experimental error. Nonetheless, stronger supportive data are desirable; these come from considering the proton profiles for immobilized BSA, and from reconsidering early data for other native proteins (Hallenga and Koenig, 1976).

### *Results from proton NMRD profiles of BSA*

Explication of the proton $1/T_1$ NMRD profiles requires inclusion of magnetization transfer at the two classes of binding sites described in the foregoing, which is readily accomplished by assigning two parameters that measure the water-protein proton-proton coupling at each class of site. For BSA, the best-fit values were found to be one and four times the proton-proton interaction in a water molecule, for the 1-$\mu$s and 23-ns sites, respectively. When these interactions are included in the theory, all the data of Fig. 1, plus newer proton data on samples with variable deuteron content (which changes the relative important of magnetization transfer compared with hydrodynamic relaxation) can be fit suitably well with only these six parameters (Koenig and Brown, 1993). In particular, the functional form of the cross-linked profile is readily explained (e.g., the hump in the proton data for the cross-linked protein in the range 0.6–6 MHz (Fig. 1) is dominated by the 23-ns sites). In addition, the relatively small contribution of magnetization transfer to $1/T_1$ for native BSA solutions and the very large contribution for cross-linked BSA (Fig. 2 of Koenig et al., 1993d) is explained as well. The theory also explains $1/T_1$ measurements for the protein protons of powdered (but wet) BSA (Schauer et al., 1988; Kimmich at al., 1986). This relatively good agreement of data and theory (Fig. 4 of Koenig and Brown, 1993) can be improved by assuming somewhat of a spread in the $\tau_M$ values at the two classes of sites and, for the low-field proton data (below 0.03 MHz), by invoking the consequences, ignored here, of the progressive overlap of broadened proton Zeeman levels in the solid-state proteins (Brown and Koenig, 1992).

### *Reinterpretation of results from proton NMRD profiles of other proteins*

Fig. 2 shows early proton $1/T_1$ profiles (Hallenga and Koenig, 1976) for 5 wt % solutions of five native proteins spanning a 30-fold range of molecular weight. For four of the five proteins, with $\nu_c$ for the NMRD profiles ranging from $\sim$0.8–8 MHz, the intrinsic 0.1 MHz $\nu_c$ associated with the 1-$\mu$s sites is sufficiently long so as not to influence the major rotation-related dispersion of each protein. But, of

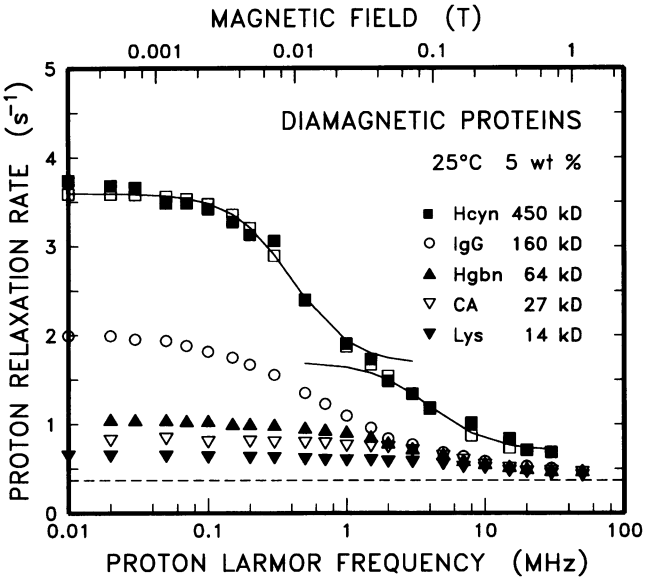


FIGURE 2 Proton $1/T_1$ NMRD profiles of water solutions of native globular proteins with a 30-fold range of molecular weights, all 5 wt %, at 25°C. The proteins are partly associated hemocyanin (■;, Hcyn, 450 kDa), bovine immunoglobulin G (○, IgG, 160 kDa), oxyhemoglobin (▲, Hgbn, 64 kDa), bovine carbonic anhydrase B (▽, CA, 27 kDa), and egg-white lysozyme (▼, Lys, 14 kDa). The solid curves associated with the Hcyn data are each single Lorentzians, with $\nu_c$ values of 0.4 and 4.0 MHz, and integrated areas in the ratio 1:5.2 respectively; their sum (□) clearly represents the Hcyn data extremely well. (The 0.4 MHz curve is shifted upward as a visual aid.) The horizontal dashed line is the contribution of solvent. (Data after Hallenga and Koenig, 1976.)

more significance, the 23-ns sites dominate the dispersion in the field decade centered near 4 MHz at which, for the four lighter proteins, the $1/T_1$ profiles have dispersed significantly. In addition, a variety of other small effects including dissolved oxygen, trace amounts of paramagnetic impurities, and the unknown contributions of the majority of the protein hydration layer help to obscure the contribution of the 23-ns sites. However, particularly in retrospect, the profile for 450 kDa hemocyanin (Hcyn) is very telling. Were there but one class of binding site that dominated the profiles for all these samples, by the nature of a Lorentzian, the Hcyn profile would have to intersect each of the other profiles at some higher field. Whether or not the other profiles, Fig. 1, cross each other at the higher fields is moot, but the Hcyn profile assuredly does not cross any of the others.

The explication in terms of 1-$\mu$s and 23-ns sites, and therefore two Lorentzians, is immediate: there is a low-field dispersion, with $\nu_c$ = 0.40 MHz, contributed by the 1-$\mu$s sites, for which $\tau_M$ is sufficiently long so that protein rotation determines $\nu_c$; and a high-field dispersion, with $\nu_c$ = 4.0 MHz, the value associated with 23 ns. (The heavier proteins appear stationary for waters bound at these sites.) The two solid curves associated with the Hcyn data (one displaced upward for clarity), with a sum indicated by open squares, are each the expected Lorentzian contributions associated with the two classes of sites, with a relative population ratio of 1:5.2 for the 1-$\mu$s and 23-ns sites, respectively. (Recall that, for BSA, the ratio is very similar, ~1:7.) The agreement of the computations with the data is the most straightforward experimental demonstration of which we are aware of the existence of 23-ns sites, here demonstrated for a protein other than BSA. However, the present reanalysis of older data was stimulated by the very recent indications of their existence in BSA (Fig. 1) (Koenig and Brown, 1993).

## MULTIPLE HYDROGEN BONDS: THE BASIS OF BINDING HETEROGENEITY

### Four-hydrogen bond sites

For protein solutions within about one pH unit of neutrality, most protein-water interfaces are very similar. Typically, $(COO)^-$ groups predominate among the negative interfacial charges, and $(NH_3)^+$ groups are the major positive charges. The few surface histidines can generally be ignored, to first order. These charged groups cover ~30% of the interfacial area, and only a few can become involved in multiple hydrogen bonding. We have previously (Koenig et al., 1993c) associated the 1-$\mu$s sites with waters held at the protein-water interface by four hydrogen bonds. The concept was that a single proton of an interfacial water bound to a $(COO)^-$ was linked, in a highly symmetric geometry, to both carboxyl oxygens, forming two hydrogen bonds, for tighter bonding. Under favorable but relatively infrequent conditions, the second water proton can bind similarly to the $(COO)^-$ of another surface amino acid, for a total of four hydrogen bonds per bound water. Although there is little precedence for this idea, neutron scattering experiments from single crystals of myoglobin (16 kDa and ~50% water) do indicate a single interfacial water in a position to form four hydrogen bonds: one proton held symmetrically between the oxygens of a surface $(COO)^-$ and the other symmetrically bridging imidazole nitrogens of two interfacial histidines (Schoenborn, 1988; Cheng and Schoenborn, 1990,1991a,b), which is equivalent in concept.

Proton $1/T_1$ NMRD profiles have been measured for solutions of several dozen native globular proteins; a summary of the data for 16 proteins, ranging over four orders of magnitude in molecular weight (cf. Fig. 4 of Koenig and Brown (1991)), shows that the surface density of the 1 $\mu$s sites is, within a factor of two, the same for all. In addition, a recent comparison of BSA with $\alpha$-crystallin (10-fold greater mass) was made, using both proton $1/T_1$ NMRD profiles and direct measurements of solute-solvent magnetization transfer (Koenig et al., 1993b, d); both sets of data show (independently) that the surface density of the 1-$\mu$s sites is the same for these two proteins, covering $\leq$1% of the interfacial area. Fewer data exist that show the variability of $\tau_M$ values; e.g., the $\tau_M$ values for carbonic anhydrase (30 kDa) and BSA (68 kDa) (cf. Fig. 2 of Koenig et al., 1993c), and myoglobin (16 kDa) (S. H. Koenig and R. Ugolini, unpublished results) are indistinguishable. Finally,

we have seen no data to indicate that there are waters held for a significantly longer time, i.e., with $\tau_M$ values in the approximate range 0.01–1 $\mu$s, and which are in rapid exchange with solvent.

A rough estimate of $\tau_M$, derived from observed vibration periods of single hydrogen bonds ($\sim 5.3 \times 10^{-14}$ s), the activation energy for their dissociation ($\sim 2.6$ kcal mol$^{-1}$), plus the admittedly simplistic assumption of relative independence (additivity) of the bonding energies of multiple bonds, gives 0.83 $\mu$s for $\tau_M$, at 35°C, in remarkable support of the fundamental and novel conjecture regarding the physical chemistry of the 1-$\mu$s sites (Koenig et al., 1993c).

One can extend these ideas to binding of waters by fewer bonds, resulting in shorter characteristic values of $\tau_M$. Table 1 shows estimated values for $\tau_M$ for protein-bound interfacial water molecules held by $n$ hydrogen bonds, for $n$ = 1,2,3,4. It is assumed that the bonds are independent and that each additional bond contributes a factor of 50 to $\tau_M$, at 35°C. The associated $\nu_c$ values are those expected for immobilized protein, as are the values of $B_0$ at which an inflection in the $1/T_1$ profiles would be seen. The actual values of $\tau_M$ for a single class of site, of course, must have some spread but, on the basis of a large amount of data, this spread is relatively small compared with the separation of the average $\tau_M$ values for different values of $n$.

## Three-hydrogen bond sites

Extending the argument, a single water proton will generally form two hydrogen bonds with an interfacial $(COO)^-$ (i.e., rarely only one, simply on arguments of symmetry and energetics), except for unusual steric restraints. For 23-ns sites (estimated at 20 ns in Table 1), the assumption (Koenig and Brown, 1993) is that these waters are held by three bonds: the usual symmetric two-bond association with a $(COO)^-$ group for one proton and, because of less favorable geometry, only a single bond for the second proton.

There has been but one report of this class of site (Koenig and Brown, 1993) before the present reexamination of older proton NMRD data (Fig. 2). A major reason is that the influence on relaxation of its sevenfold greater site density, compared with the four-bond sites, is readily offset by its 50-fold shorter $\nu_c$ (for immobilized protein and more so for native material), so that the contribution to $1/T_1$ of protein solutions is generally small and unimportant. Their density, too, is quite low: $\leq$2% of the interfacial area.

Two recent studies of protein solutions, using high-resolution two-dimensional (2D) NMR, lend support to the foregoing ideas; i.e., the existence of a few hydration waters with long values of $\tau_M$. In one report, a protein-oligo-DNA complex (Qian et al., 1993, p. 1190), the authors found "only very few [long-lived] water molecules hydrating the . . . complex" and "have well established that the few . . . waters are . . . in the interface between the protein and the DNA." In another, an HIV protease (Grzesiek et al., 1994, p. 1582), the authors report "the presence of such a [long-lived] water in the immediate vicinity of the substrate binding site of HIV protease." For both examples, the water-binding sites are few and clearly special. Unfortunately, such experiments do not yield even approximate values for $\tau_M$: $2 \times 10^{-2} \leq \tau_M \leq 10^{-9}$ s for the protein-DNA complex and $10^{-1} \leq \tau_M \leq 2 \times 10^{-9}$ s for the protease.

**TABLE 1 Values of $\tau_M$, the lifetime of a water molecule bound at a protein-water interfacial site, when held by $n$ hydrogen bonds, at 25°C**

| $n$ | $\tau_M$ (s) | $\nu_c \approx 1/11\tau_M$ (MHz) | $B_0$ (T) |
|---|---|---|---|
| 4 | $1 \times 10^{-6}$ | 0.1 | 0.0024 |
| 3 | $2 \times 10^{-8}$ | 5 | 0.12 |
| 2 | $4 \times 10^{-10}$ | 250 | 6 |
| 1 | $8 \times 10^{-12}$ | 12,500 | 300 |

For solutions of immobilized protein, every value of $\tau_M$ determines a value of $\nu_c$ (Koenig and Brown, 1991), the correlation frequency of a distinct Lorentzian contribution to the $1/T_1$ NMRD profiles of solvent protons, with an inflection at $B_0$.

## Two-hydrogen bond sites

One fewer bond corresponds to shortening $\tau_M$ about 50-fold. Thus, a water held by only two bonds should have $\tau_M$ $\sim$450 ps. There is certainly evidence for a significant number of interfacial sites with lifetimes close to this value. One example, from early work, derives from the values of $1/T_1$ in protein solutions at high fields, well above the major lower field dispersions (Koenig and Schillinger, 1969; Koenig, 1980), which yields just this value for $\tau_M$, and a site-density $\sim$30% of the interfacial area (Koenig, 1980).

A second example comes from analysis of relaxation at the myelin-water interface of white matter of adult brain. The argument is somewhat less germane because the macromolecule in question is a phospholipid bilayer which, for myelin, has a surface dense with the alcohol OH groups of the many structural cholesterol molecules of myelin; it is hydrogen bonding of myelin water to these sites (Koenig et al., 1990; Koenig, 1991), and possibly others surface hydroxyls (Ceckler et al., 1992), which ultimately makes adult white matter brighter than gray matter in MRI. Again, the estimate is $\tau_M$ $\sim$400 ps (assuming 50% coverage by hydroxyl groups) which, retrospectively, would also arise from waters held by two hydrogen bonds.

A third example is the more recent study, by high field, high resolution, multidimensional NMR, of protein-water proton-proton interactions, using the small (7 kDa) protein bovine pancreatic trypsin inhibitor (Otting and Wüthrich, 1989; Otting et al., 1991). Again, a similar $\tau_M$ was estimated from the absolute rate of magnetization transfer (Overhauser effect) observed between solute and solvent, assuming that water-protein geometries were sufficiently well known to make these calculations reliable. A protein this small, statistically, may have no 1-$\mu$s sites, or even 23-ns sites, and none was reported; the heterogeneity of water-

binding sites on proteins in general was missed in this work, although two-bond sites abound. Consistent with the trypsin inhibitor data are the results for the protein-DNA complex (Qian et el., 1993, p. 1190), for which the authors find "that the residence times of water molecules in the surface hydration sites are shorter than about 0.5 ns." However, it should be noted that such Overhauser data are difficult to obtain, and a recent molecular dynamics study of the hydration of the trypsin inhibitor (Brunne et al., 1993, p. 1046) suggests that 450 ps (with $\nu_c$ near 220 MHz) may well be an overestimate for a representative hydration water: "the effective residence times, on average, are of the order of a few tens of picoseconds." However, many instances of $\tau_M$ in the 100–500 ps range are reported (cf. Table 3 of Brunne at al., 1993) and, given that the contribution to $1/T_1$ of each bound water is weighted by its $\tau_M$, these sites indeed exist in sufficient numbers to account for the high field dispersion of $1/T_1$ of water protons in protein solutions that, as noted, centers near 250 MHz.

### One-hydrogen bond sites

From Table 1, $\tau_M$ for one-bond sites would be very short, about three times the rotational relaxation time of individual water molecules free in solution; the associated value of $\nu_c$ is too high to be studied by either NMR or NMRD methods. However, these sites could be investigated by electron spin resonance techniques. To date, there are few data to indicate the density or nature of the expected one-bond sites. Perhaps the fivefold slowing of a monolayer of water molecules in montmorillinite clay suspensions (Woessner, 1980) relates to binding of water, by a single hydrogen bond, to the oxygen-rich surface of this clay. Possibly the highly regular interfacial geometry of these particular clays precludes the stronger binding found in proteins. Interestingly, the high-resolution NMR results for the trypsin inhibitor (Otting et al., 1991) are on average like that for clay; they give an interfacial diffusion constant for hydrations waters fourfold lower than that of pure water.

As a final point, one-bond binding of water, oxygen first, to highly polar OH groups, e.g., or to positive interfacial charges has not been considered here. For cross-linked protein, e.g., the $(NH_3)^+$ groups become blocked, and the point is moot. For tissue, more data and more thought are needed.

## RELEVANCE TO MRI

### The $(1/T_2)/(1/T_1)$ ratio, generally

$1/T_1$ NMRD profiles have dominated the foregoing review; $1/T_2$ profiles, or even $1/T_2$ values, are rarely mentioned. The reason is simple: it is technically difficult to measure $1/T_2$ in a field-cycling relaxometer, and few such data exist. Fortunately (as noted above), for isotropic liquids, even for those containing immobile protein, $1/T_1$ and $1/T_2$ become equal at low fields and, with a reasonable understanding of the system at hand, the $1/T_2$ profile can be inferred from the $1/T_1$ profile.

For diagnostic imaging, $B_0$ is generally in the range 1–90 MHz (0.025–1.5 T) where, for most tissues, $(1/T_2)/(1/T_1) \sim 10{:}1$. The contribution of the 1-$\mu$s sites to $1/T_1$ (cf. Fig. 1) has become negligible over this entire field range, and that of the 23-ns sites is substantially gone above ~10 MHz. Thus, for the MRI field range, $1/T_1$ is small, dominated by interactions with high $\nu_c$ values, and diluted by the natural water background. On the other hand, $1/T_2$ is roughly independent of $B_0$ in the MRI range and its values about 10-fold larger, about the same as the low field (0.01 MHz) $1/T_1$; hence the 10:1 ratio. As a result, clinically acceptable images, and greater patient throughput, can be obtained by repeating instrumental pulse sequences after intervals of several multiples of $T_2$, despite the concomitant loss of signal due to partial saturation of the proton Zeeman system. Given the goal that understanding of image contrast at the molecular level will contribute to understanding the relation of disease to alterations in MRI contrast, a full theory of $1/T_1$ NMRD profiles of tissue plus associated data can lead to understanding of $1/T_2$ in tissue in the imaging range and, hopefully, improve the diagnostic utility of MRI. A major first step, however, is to explain why samples of immobilized protein are such good models of the relaxation behavior of tissue water.

### The protein model for tissue

First, we remark once again that proton $1/T_1$ NMRD profiles of most tissues are similar to each other and to those of immobilized protein. This is also true for astrocytomas (brain tumors) (Spiller et al., 1994), other tumors, and packets of liver cells (Koenig and Brown, 1987), but not for whole blood, which has the same protein content as most tissues. The majority of blood protein (hemoglobin) is in the red cells, which in turn must have a fairly complex array of organized protein to maintain the highly toroidal cellular shape of red cells. Nonetheless, the hemoglobin of red cells is mobile, with the same rotational freedom as a solution of hemoglobin of the same concentration (Lindstrom and Koenig, 1974; Lindstrom et al., 1976). Thus, it is not the density of cellular protein that determines its rotational freedom in cells and, therefore, in tissue. Rather, other principles must be active; we have conjectured such: cytoplasmic order and cytoplasmic chaos (Koenig, 1994; Spiller et al., 1994).

#### *Cytoplasmic order*

The roles of the cells of most tissue are far more complex than simply the packaging of a carrier-protein, as for red cells. Indeed, each of the complex sequences of protein-mediated reactions required for respiration, catabolism, metabolism, cell division, genetic transcription, etc., requires clusters of many different proteins in association with each other and with membrane. Moreover, it is known that genes

for the many proteins involved in such complex reactions are often located together on the DNA and expressed as a group. In addition, there is rarely sufficient lipid in any cell type to form the amount of membrane needed to organize all protein molecules individually either on, or within, lipid bilayer membranes, into a rigid 2D structure. Accordingly, it is not outrageous, then, to conjecture that those proteins needed for a given complex function self-assemble into rather large, extended, 3D, stereospecifically organized complexes, perhaps anchored to membrane at key sites, to allow enzyme-mediated processes to progress more efficiently and to prevent one functional group from interfering with all others.

We have named this conjecture "cytoplasmic order"; without some (evolution-driven?) refinement of the 3D cytoplasmic organization of proteins by class of function, there will be interference between functional groups and concomitant loss of cellular efficiency. Recall that 20 wt % globular protein corresponds to a surface-to-surface separation of less than one protein diameter; the cytoplasm is a crowded place! Nonetheless, the diffusion of water in these crowded cells is, within a factor of two, that of pure water, and the rotation of hemoglobin is as if it were free in solution. Given that $1/T_1$ profiles for immobilized protein (with rotational relaxation times corresponding to globular proteins with molecular weights $\geq 5 \times 10^7$ Da) and for tissue are indistinguishable, the immediate inference is that the proteins in the cytoplasm, organized by functional groups, must be correspondingly rigid (if not correspondingly closely packed). Moreover, from experience with measurements on many samples, one can estimate that most of the cytoplasmic protein ($\geq$75%) is so organized. This is the basis of contrast in MRI.

We emphasize that cytoplasmic order is not the result of an extensive cytoskeleton in some (many, all?) cells. That is too facile an explanation of the similarity of the NMRD profiles of tissue and immobile protein; there is too little protein in the cytoskeleton as there is too little lipid to explain the motional restriction on essentially all cytoplasmic protein. As an aside, an interesting pictorial example of such cytoplasmic order was reported recently for the complex dynamics of platelet receptor expression and fibrinogen binding (cf. Fig. 1 of Frojmovic et al., 1994). A second (cf. Peifer, 1993) shows an extended complex of plasma membrane and catenins in turn linked with actin cytoskeleton.

### *Cytoplasmic chaos*

The major goal of clinical MRI is diagnostic: to discover pathology, including neoplastic transformation (cancer), in tissue. The intriguing question is, of course, whether there can be a marker of relaxation behavior in tumors related to the extent of such transformation. This has been difficult to demonstrate, despite early claims, because of the need to normalize the data for solids content of the tissue, and to eliminate (at least initially) tumors containing hemorrhage and calcifications, each with its own contribution to $1/T_1$. However, using rigorous histological controls, it was recently possible to demonstrate (Spiller et al., 1994) the existence of a parameter in human astrocytomas that influences their $1/T_1$ NMRD profiles and which, on average, increases with the grade of malignancy of the tumor. A conjectured mechanism (Koenig, 1994) was the progressive breakdown of the fine-tuned cytoplasmic order to a state of "cytoplasmic chaos." At cellular protein concentrations, the protein-protein hydrodynamic interactions are generally large and very sensitive to the mean-squared protein separation (for fixed total protein). An increase in cytoplasmic chaos, leading to more net crowding of cell protein, alters NMRD profiles in a direction consistent with a greater influence of solid state effects related to the progressively slowed protein. The correlation is certainly there for high grade (more malignant) astrocytomas, and the explanation in terms of cytoplasmic chaos has the advantage and attraction of being based on a broad principle, hopefully of broad applicability in MRI. (For the highest grade astrocytomas, the nuclei become so large that "cellular chaos" may be a better term.) In support of the foregoing is the recent finding that, for meningiomas, the most benign and slow-growing of brain tumors, there is little indication of an elusive parameter, expressed either in NMRD profiles or in MRI, that correlate with neoplasticity (Kasoff et al., 1995).

## DISCUSSION

Relaxation processes are of necessity dissipative, involving energy exchange between a given degree of freedom of an ensemble (here, the macroscopic magnetization of solvent nuclei) and the greater thermal reservoir of energy (that, here, comprises the solvent as "lattice"). For example, if all encounters of solvent with solute were nondissipative, there could be no contribution to the longitudinal relaxation of solvent nuclei; i.e., no exchange of Zeeman energy between the nuclear ensemble and the water and protein thermal reservoirs. As a supportive example, $1/T_1$ of water in 20% polyacrylamide gel (S. H. Koenig and M. Spiller, unpublished data), a hard rigid solid, is about the same as in pure water; here, an abundant interface lacking water-binding sites with a long $\tau_M$ (which makes interfacial encounters highly dissipative) has little measurable influence on solvent $1/T_1$ at any value of $B_0$. By contrast, the influence of protein-water encounters on the relaxation rates of water nuclei is large, a reflection of the presence of dissipative interactions. By the nature of motional narrowing, the lower the magnitude of $\nu_c$, the more loss in the encounters; hence the amplification, often by very large factors, of the influence of sites with long values of $\tau_M$ when conditions are such that $\tau_M$ determines $\nu_c$. As already noted, this amplification can be $10^6$-fold or more, leading to complex and useful relaxation properties, but with little influence of these dissipative encounters on the gross motion of the solvent water molecules.

It is fair to say that a water molecule must come within its own diameter (~3 Å) of an interface to sense its presence. For protein-water interfaces, ~60–70% of the interfacial area acts as little more than as an impenetrable surface, resulting in "hard," nondissipative, encounters: extrapolating from data for clay (Woessner, 1980), this interfacial region can be modeled as a single hydration layer in which water may be slowed as much as fivefold if a single hydrogen bond is formed during an encounter, and less otherwise. In another ~30% of the area, particularly near negatively charged carboxyls, waters are held sufficiently long (~400 ps) that their effect can be modeled as a 100-fold slowing of a monolayer of water. But it is the remaining 2% or less of the interface that includes the classes of binding sites that are important in the relaxometry of protein and of tissue, and determines contrast in MRI. These include the 1-$\mu$s and 23-ns sites at which the long $\tau_M$ values of bound waters exaggerate the minor influence of this binding on the average molecular dynamics of water, to dominate solvent and solute proton relaxation.

The $\tau_M$ weighting of the contribution of a class of interfacial sites to solvent nuclear $1/T_1$ and $1/T_2$ makes the simple modeling of interfacial relaxation and magnetization transfer—often by a single parameter unlinked from mechanism and meant to "typify" the interface—of dubious utility, particularly if the goal is to gain understanding at the molecular level. For example, in a recent analysis of relaxation in protein systems (Zhou and Bryant, 1994), the functional form of the NMRD profile was simply assumed rather than derived from interfacial mechanisms, and values for descriptive rather than mechanistic parameters were then obtained. In another example (Ceckler et al., 1992), magnetization transfer was measured at 200 MHz in suspensions of lipid bilayers, in solutions of polysaccharides and proteins, and in tissue, which all have differing interfacial structures. Although they noted "that the hydroxyl and amine groups serve as hydrogen bonding sites, the lifetime being on the order of microseconds," (p. 643) this is really a guess. The actual data give $\tau_M \gg 10^{-9}$ s: from data at one value of $B_0$ (i.e., with no NMRD profile), one cannot distinguish a few sites with very long $\tau_M$ values from many sites with a much shorter $\tau_M$.

Finally, and in another vein, because the 1-$\mu$s, four-bond sites are relatively sparce—with a mean tissue density ~5 mM—it might be possible to design nontoxic stereospecific pharmaceutical agents that can compete with water molecules for these sites, deenhancing significantly MRI contrast in a manner that is clinically advantageous.

*Note added in proof*—It is only after submission of this work that the author become aware of a corpus of research on protein solutions at high concentrations that complements the present work; the thermodynamic aspects, both theoretical and experimental, are in a recent review by Zimmerman and Minton (1993).

## REFERENCES


Beaulieu, C. F., R. D. Brown III, J. I. Clark, M. Spiller, and S. H. Koenig. 1989. Relaxometry of lens homogenates. II. Temperature dependence and comparison with other proteins. *Magn. Reson. Med.* 10:362–372.

Bloembergen, N., E. M. Purcell, and R. V. Pound. 1948. Relaxation effects in nuclear magnetic resonance absorption. *Phys. Rev.* 73:679–712.

Brown III, R. D., and S. H. Koenig. 1992. $1/T_{1\rho}$ and low field $1/T_1$ of tissue water protons arise from magnetization transfer to macromolecular solid-state broadened lines. *Magn. Reson. Med.* 28:145–152.

Brunne, R. M., E. Liepinsh, G. Otting, K. Wüthrich, and W. F. van Gunsteren. 1993. Hydration of proteins. A comparison of experimental residence times of water molecules solvating the pancreatic trypsin inhibitor with theoretical model calculations. 1993. *J. Mol. Biol.* 231: 1040–1048.

Bryant, R. G., D. A. Mendelson, and C. C. Lester. 1991. The magnetic field dependence of proton spin relaxation in tissues. *Magn. Reson. Med.* 21:117–126.

Ceckler, T. L., S. D. Wolff, V. Yip, S. A. Simon, and R. S. Balaban. 1992. Dynamic and chemical factors affecting water proton relaxation by macromolecules. *J. Magn. Reson.* 98:637–645.

Cheng, X., and B. P. Schoenborn. 1990. Hydration in protein crystals. A neutron diffraction study of carbonmonoxymyoglobin crystals. *Acta Crystallogr.* B46:195–208.

Cheng, X., and B. P. Schoenborn. 1991a. Repulsive restraints for hydrogen bonding in least-squares refinement of protein crystals. A neutron diffraction study of myoglobin crystals. *Acta Crystallogr.* A47:314–317.

Cheng, X., and B. P. Schoenborn. 1991b. Neutron diffraction study of carbonmonoxymyoglobin. *J. Mol. Biol.* 220:381–399.

Daszkiewicz, O. K., T. W. Hennel, B. Lubas, and T. W. Szczepkowski. 1963. Proton magnetic relaxation and protein hydration. *Nature (Lond.)* 200:1006–1007.

Frojmovic, M. M., R. F. Mooney, and T. Wong. 1994. Dynamics of platelet glycoprotein receptor IIa-IIIb receptor expression and fibringen binding. I. Quantal activation of platelet subpopulations varies with adenosine diphosphate concentration. *Biophys. J.* 67:2060–2068.

Grzesiek, S., A. Bax, L. K. Nicholson, T. Yamazaki, P. Wingfield, S. J. Stahl, C. J. Eyermann, D. A. Torchia, C. N. Hodge, P. Y. S. Lam, P. K. Jadhav, and C.-H. Chang. 1994. NMR evidence for the displacement of a conserved interior water molecule in HIV protease by a non-peptide cyclic urea-based inhibitor. *J. Am. Chem. Soc.* 116:1581–1582.

Hallenga, K., and S. H. Koenig. 1976. Protein rotational relaxation as studied by solvent $^1$H and $^2$H magnetic relaxation. *Biochemistry.* 15: 4255–4264.

Kasoff, S. S., M. Spiller, M. P. Valsamis, T. A. Lansen, K. R. Duffy, S. H. Koenig, and M. S. Tenner. 1995. Relaxometry of non-calcified human meningiomas. Correlation with histology and solids content. *Invest. Radiol.* 30:49–55.

Kimmich, R., F. Winter, W. Nusser, and K.-H. Spohn. 1986. Interactions and fluctuations deduced from proton field-cycling relaxation spectroscopy of polypeptides, DNA, muscles, and algae. *J. Magn. Reson.* 68: 263–282.

Koenig, S. H. 1980. The dynamics of water-protein interactions: results from measurements of nuclear magnetic relaxation dispersion. *In* Water in Polymers. Stanley P. Rowland, editor. *ACS Symp. Ser.* 127:157–176.

Koenig, S. H. 1988. Theory of relaxation of mobile water protons by protein NH moieties, with application to rat heart muscle and calf lens homogenates. *Biophys. J.* 53:91–96.

Koenig, S. H. 1991. Cholesterol of myelin is the determinant of gray-white contrast in MRI of brain. *Magn. Reson. Med.* 20:285–291.

Koenig, S. H. 1994. Cytoplasmic order and cytoplasmic chaos: why immobilized proteins in water solutions are good models for relaxation of water proteins of tissue. *Proc. Soc. Magn. Reson., Vol. 2, San Francisco, CA. 893.*

Koenig, S. H., and R. D. Brown III. 1985. The importance of the motion of water for magnetic resonance imaging. *Invest. Radiol.* 20:297–305.

Koenig, S. H., and R. D. Brown III. 1987. Relaxometry of tissue. *In* NMR Spectroscopy of Cells and Organisms. Vol. II. R. K. Gupta, editor. CRC Press, Boca Raton. 75–114.

Koenig, S. H., and R. D. Brown III. 1988. The raw and the cooked: or the importance of the motion of water for MRI, revisited. *Invest. Radiol.* 23:495–497.

Koenig, S. H., and R. D. Brown III. 1991. Field-cycling relaxometry of protein solutions and tissue: implications for MRI. *Prog. NMR Spectrosc.* 22:487–565.

Koenig, S. H., and R. D. Brown III. 1993. A molecular theory of relaxation and magnetization transfer: application to cross-linked BSA, a model for tissue. *Magn. Reson. Med.* 30:685–695.

Koenig, S. H., R. D. Brown III, D. Adams, D. Emerson, and C. G. Harrison. 1984. Magnetic field dependence of $1/T_1$ of protons in tissue. *Invest. Radiol.* 19:76–81.

Koenig, S. H., R. D. Brown III, A. K. Kenworthy, A. D. Magid, and R. Ugolini. 1993a. Intermolecular protein interactions in solutions of bovine $\beta_L$-crystallin: results from $1/T_1$ magnetic relaxation dispersion profiles. *Biophys. J.* 64:1178–1186.

Koenig, S. H., R. D. Brown III, M. Spiller, B. Chakrabarti, and A. Pande. 1992. Intermolecular protein interactions and conformation change in solutions of calf lens $\alpha$-crystallin: results from $1/T_1$ profiles. *Biophys. J.* 61:776–785.

Koenig, S. H., R. D. Brown III, A. Pande, and R. Ugolini. 1993b. Rotational inhibition and magnetization transfer in $\alpha$-crystallin solutions. *J. Magn. Reson. B.* 101:172–177.

Koenig, S. H., R. D. Brown III, M. Spiller, and N. Lundbom. 1990. Relaxometry of brain: why white matter appears bright in MRI. *Magn. Reson. Med.* 14:482–495.

Koenig, S. H., R. D. Brown III, and R. Ugolini. 1993c. A unified view of relaxation in protein solutions and tissue, including hydration and magnetization transfer. *Magn. Reson. Med.* 29:77–83.

Koenig, S. H., R. D. Brown III, and R. Ugolini. 1993d. Magnetization transfer in cross-linked bovine serum albumin solutions at 200 MHz: a model for tissue. *Magn. Reson. Med.* 29:311–316.

Koenig, S. H., R. G. Bryant, K. Hallenga, and G. S. Jacob. 1978. Magnetic cross-relaxation among protons in protein solutions. *Biochemistry.* 17: 4348–4358.

Koenig, S. H., K. Hallenga, and M. Shporer. 1975. Protein-water interaction studied by solvent $^1H$, $^2H$, and $^{17}O$ magnetic relaxation. *Proc. Natl. Acad. Sci. USA.* 72:2667–2671.

Koenig, S. H., and W. E. Schillinger. 1969. Nuclear magnetic relaxation dispersion in protein solutions I. Apotransferrin. *J. Biol. Chem.* 244: 3283–3289.

Lester, C. C., and R. G. Bryant. 1991. Water-proton nuclear magnetic relaxation in heterogeneous systems: hydrated lysozyme results. *Magn. Reson. Reson.* 22:143–153.

Lindstrom, T. R., and S. H. Koenig. 1974. Magnetic-field-dependent water proton spin-lattice relaxation rates of hemoglobin solutions and whole blood. *J. Magn. Reson.* 15:344–353.

Lindstrom, T. D., S. H. Koenig, T. Boussios, and J. F. Bertles. 1976. Intermolecular interactions of oxygenated sickle hemoglobin in cells and cell-free solutions. *Biophys. J.* 19:679–689.

Noack, F. 1986. NMR field-cycling spectroscopy: principles and applications. *Prog. NMR Spectrosc.* 18:171–276.

Otting, G., and Wüthrich, K. 1989. Studies of protein hydration in aqueous solution by direct NMR observation of individual protein-bound molecules. *J. Am. Chem. Soc.* 111:1871–1888.

Otting, G., E. Liepinsh, and K. Wüthrich. 1991. Protein hydration in aqueous solution. *Science.* 254:974–980.

Peifer, M. 1993. Cancer, catenins, and cuticle pattern: a complex connection. *Science.* 262:1167–1668.

Qian, Y. Q., G. Otting, and K. Wüthrich. 1993. NMR detection of hydration water in the intermolecular interface of a protein-DNA complex. *J. Am. Chem. Soc.* 115:1189–1190.

Redfield, A. G., W. Fite, and H. E. Bleich. 1968. Precision high speed current regulators for occasionally switched inductive loads. *Rev. Sci. Instrum.* 39:710–715.

Schauer, G., R. Kimmich, and W. Nusser. 1988. Deuteron field-cycling relaxation spectroscopy and translational water diffusion in protein. *Biophys. J.* 53:397–404.

Schoenborn, B. P. 1988. Solvent effect in protein crystals. *J. Mol. Biol.* 201:741–749.

Solomon, I. 1955. Relaxation processes in a system of two spins. *Phys. Rev.* 99:559–565.

Spiller, M., S. S. Kasoff, T. A. Lansen, S. Rifkinson-Mann, M. P. Valsamis, S. H. Koenig, and M. S. Tenner. 1994. Variation of the magnetic relaxation rate $1/T_1$ of water protons with magnetic field strength (NMRD Profile) of untreated, noncalcified, human astrocytomas: correlation with histology and solids content. *J. Neuro-Oncol.* 21:113–125.

Winter, F., and R. Kimmich. 1982a. Spin lattice relaxation of dipole nuclei ($I = 1/2$) coupled to quadrupole nuclei ($S = 1$). *Mol. Phys.* 45:33–49.

Winter, F., and R. Kimmich. 1982b. NMR field-cycling relaxation spectroscopy of bovine serum albumin, muscle tissue, *micrococcuc luteus*, and yeast. $^{14}N^1H$ dips. *Biochim. Biophys. Acta.* 719:292–298.

Woessner, D. E. 1980. An NMR investigation into the range of the surface effect on the rotation of water molecules. *J. Magn. Reson.* 39:297–308.

Zhou, D., and R. G. Bryant. 1994. Magnetization transfer, cross-relaxation, and chemical exchange in rotationally immobilized protein gels. *Magn. Reson. Med.* 32:725–732.

Zimmerman, S. B., and A. P. Minton. 1993. Molecular crowding: biochemical, biophysical, and physiological consequences. *Annu. Rev. Biophys. Biomol. Struct.* 22:27–65.